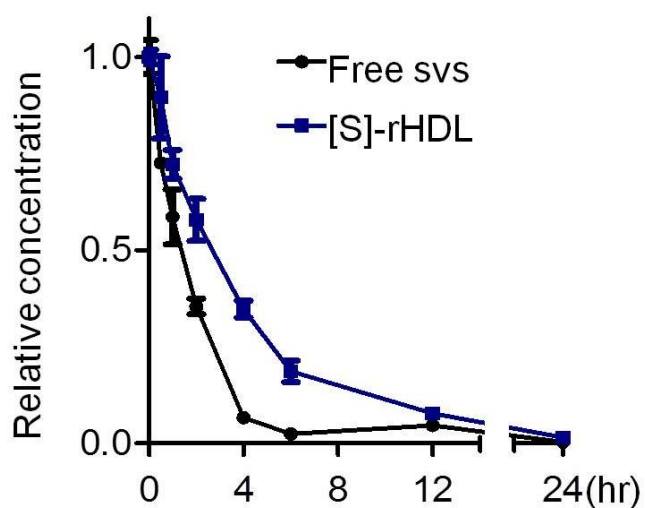
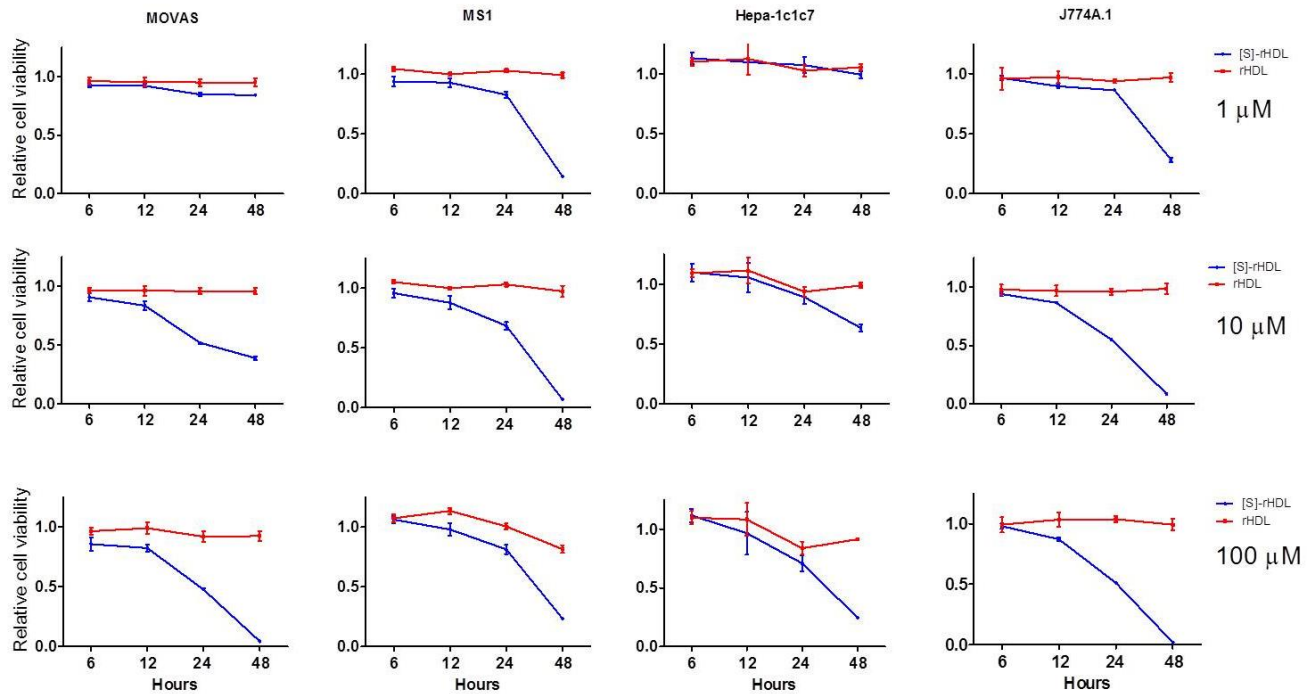


Supplementary Figure S1. Transmission electron microscopy images of negatively-stained nanoparticles. The circular shapes are nanoparticles viewed en face, while the striped configurations are rouleaux of nanoparticles viewed from the side.

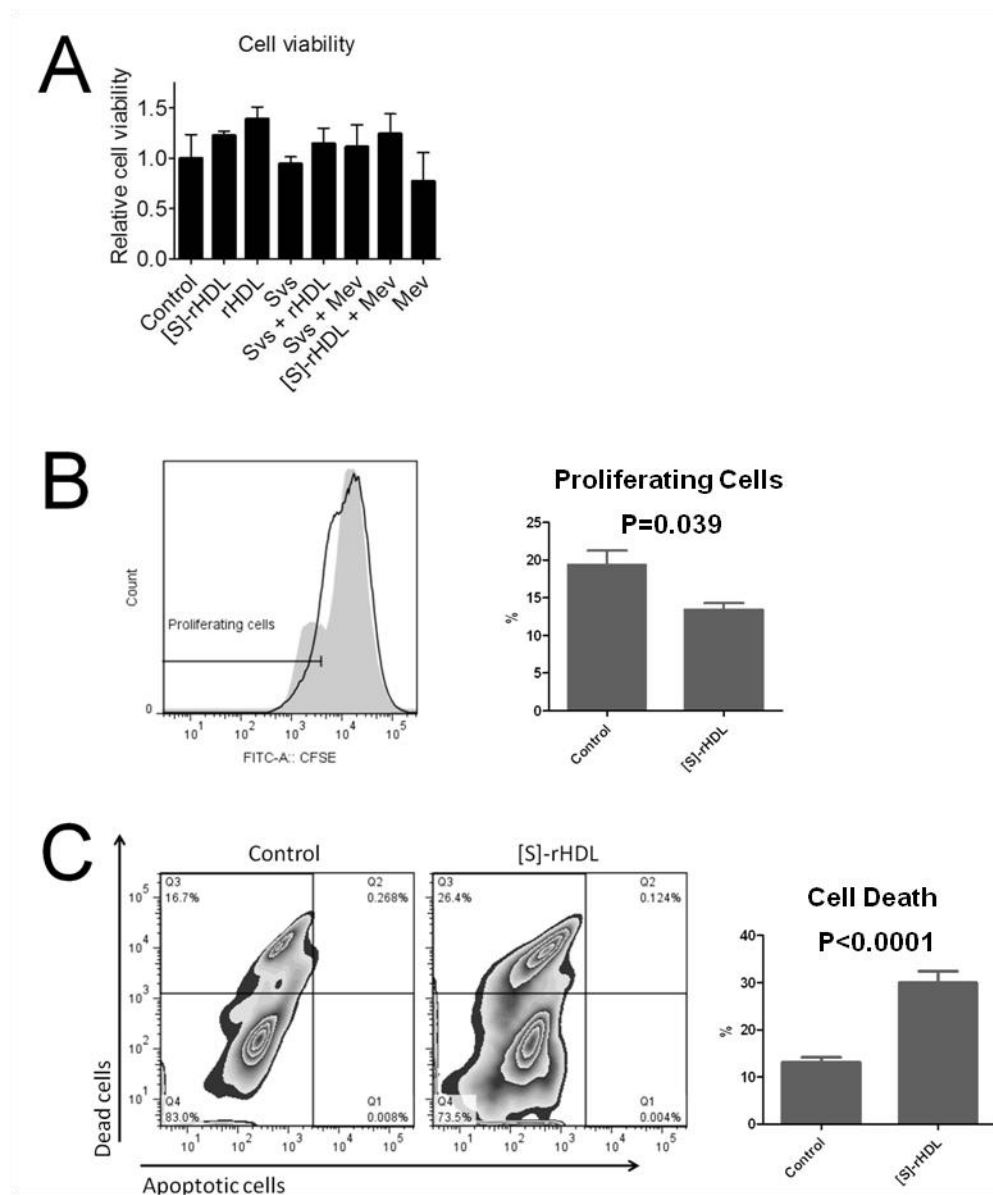


Supplementary Figure S2. [S]-rHDL has protective effects on encapsulated simvastatin in mouse serum. Relative concentration of intact simvastatin in mouse serum over time was calculated based on the measurements by HPLC compared to the initial concentration at hour 0. Each time point has 3 repeats, and error bars are standard deviations (N=3 per timepoint).

Cell viability

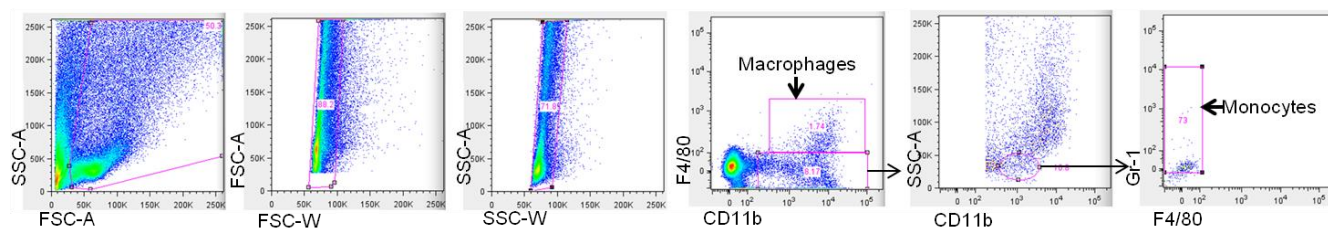


Supplementary Figure S3. Survival of different cell types in response to [S]-rHDL. Murine smooth muscle cells (MOVAS), endothelial cells (MS1), liver cells (Hepa-1c1c7), and macrophages (J774A.1) were incubated with different concentrations of [S]-rHDL as determined by simvastatin concentration in μM as well equivalent concentration of ApoA-1 delivered by rHDL *in vitro*. Cell viability was measured over time, and it was shown by comparing to the viability of cells without any treatments. Each time point has 6 repeats, and error bars are standard deviation.

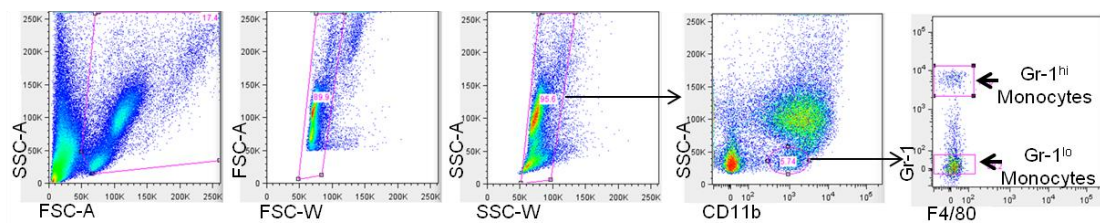


Supplementary Figure S4. (a) Murine macrophages (J774A.1) were stimulated with LPS and INF- γ for 16 hours, and subsequently treated with different treatments for 24 hours in serum-free condition. Cell viability was measured after the treatments while supernatant was used to measure the concentrations of MCP-1 and TNF- α (Fig. 2c). (b) Murine macrophages (J774A.1) were labelled with CFSE and treated with [S]-rHDL (dark line) or nothing (grey) for 24 hours. This shows that [S]-rHDL decreases macrophage cell proliferation. (c) Murine macrophages (J774A.1) were treated with [S]-rHDL for 24 hours and subsequently stained for Propidium Iodide (a cell death stain) and YO-PRO-1 (an apoptosis stain). This shows that [S]-rHDL causes non-apoptotic cell death. Error bars are standard deviations of 6 repeats. Student t-test was used to calculate statistical significance.

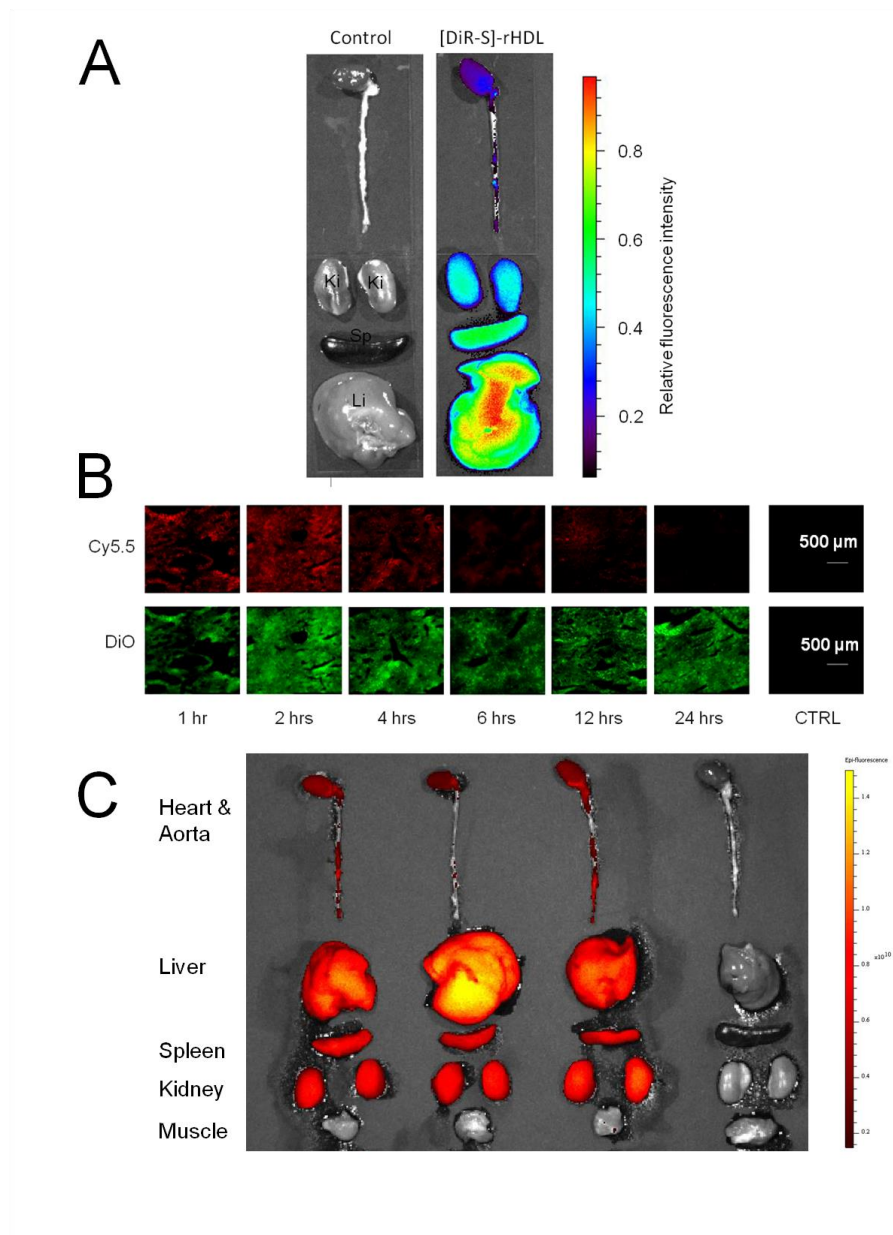
Aortas



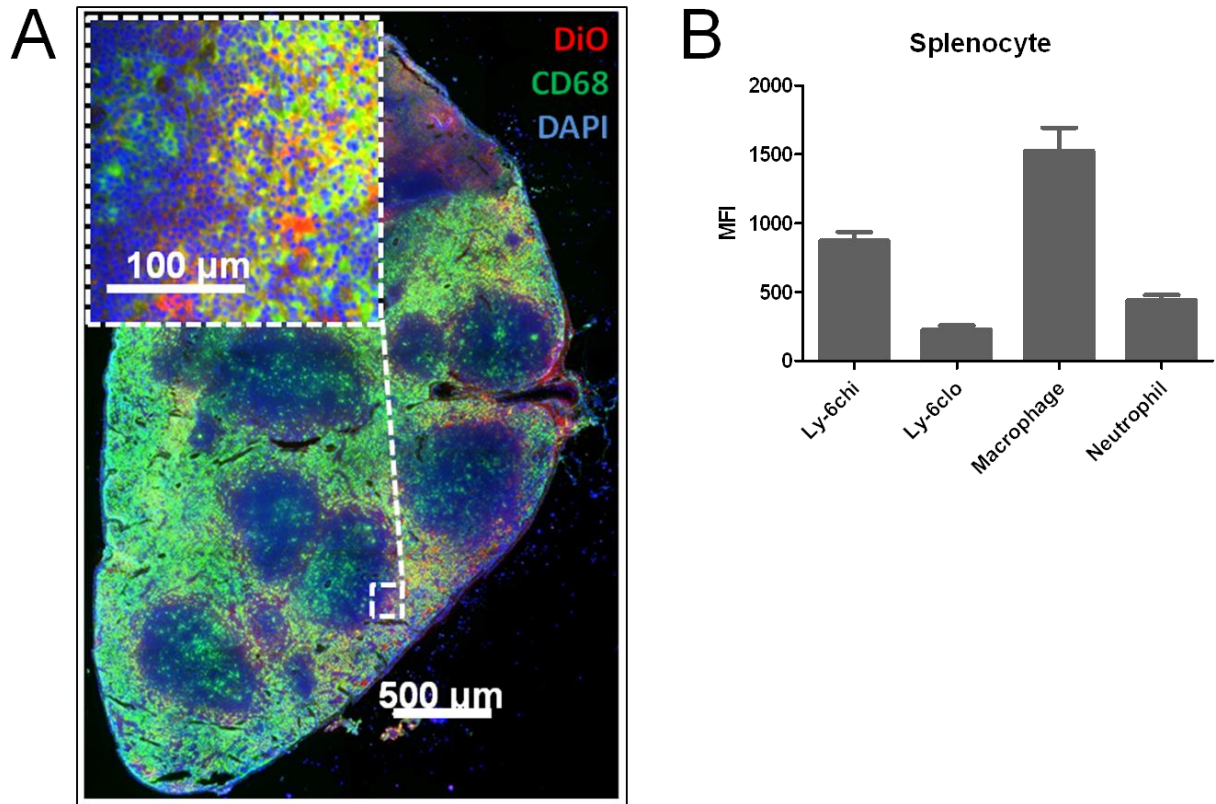
Blood



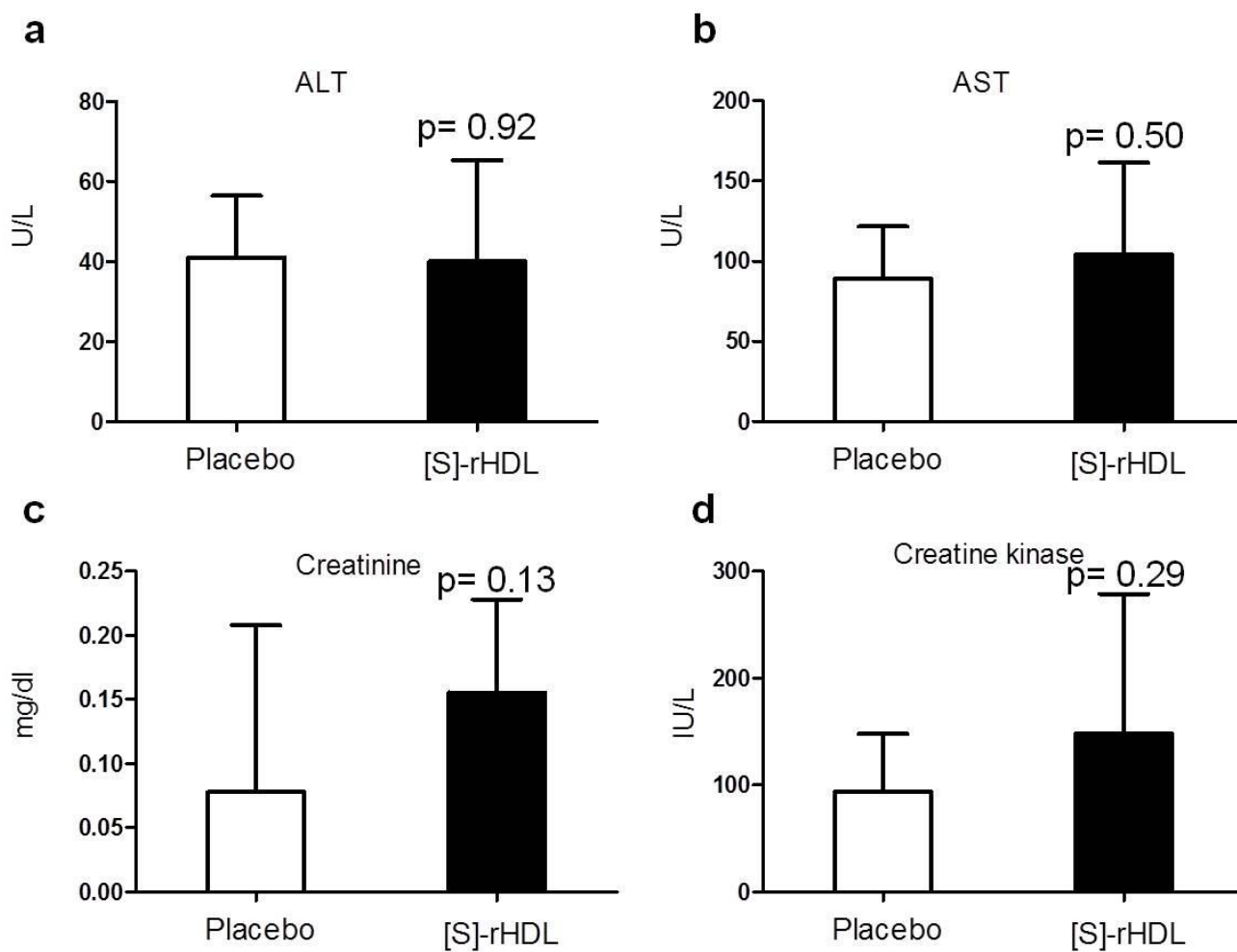
Supplementary Figure S5. Gating procedures to identify macrophages and monocytes in aortas (upper panel) and subpopulations of monocytes in blood (lower panel).



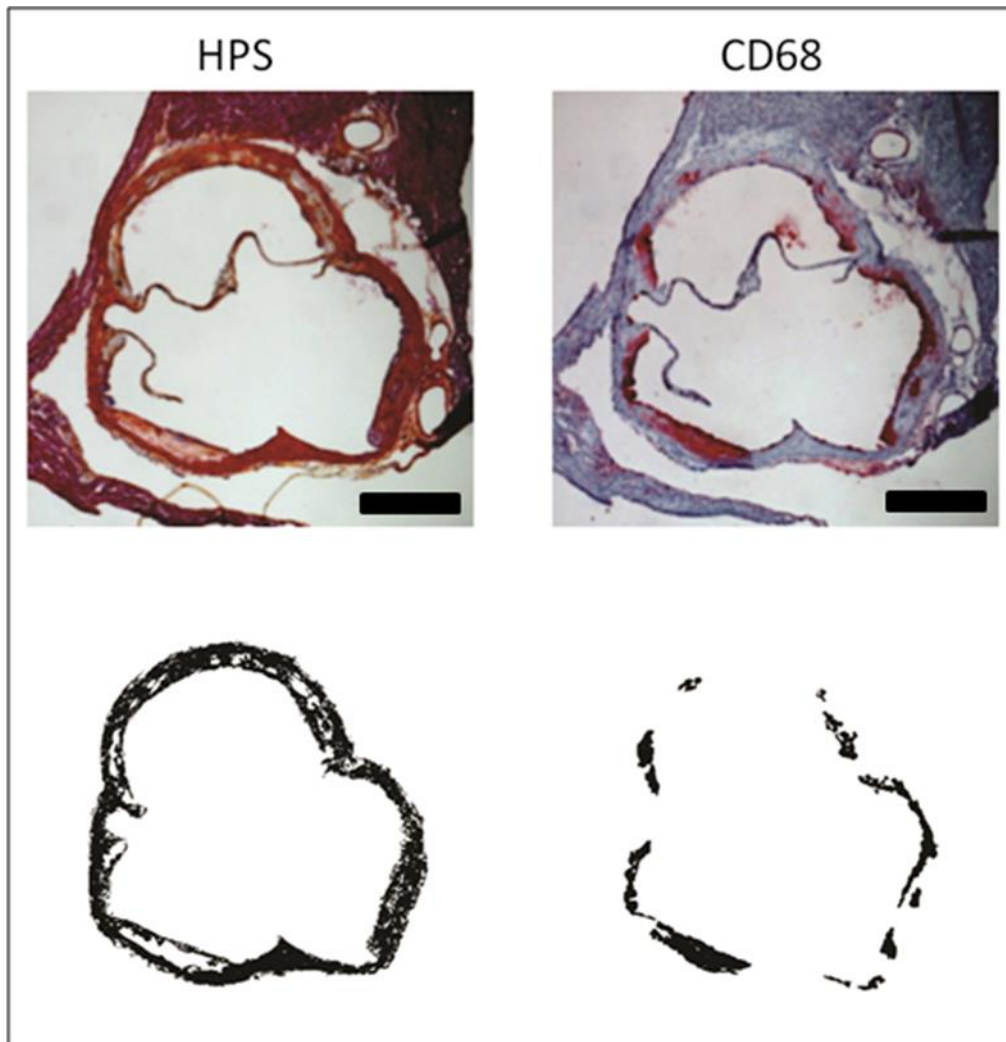
Supplementary Figure S6. Biodistribution and kinetics of hydrophobic cargo delivered by [S]-rHDL. (a) Mice were intravenously injected with [DiR-S]-rHDL nanoparticles, and organs were imaged with NIRF 24 hours after the injection. Liver has the highest retention of DiR, followed by spleen, and kidney has the lowest retention. (b) Mice were intravenously injected with [Cy5.5-DiO-S]-rHDL, and the liver retention of Cy5.5 and DiO was investigated with fluorescence microscopy at different time points after the injection. Representative images from one of 3 animals per time point are shown here. (c) Three mice were intravenously injected with [DiR-S]-rHDL (left three) and one control mouse was not injected (on the right). Organs were imaged with NIRF 24 hours after the injection. While heart, aorta, liver, spleen, and kidney tissue all took up nanoparticles, muscle tissue did not.



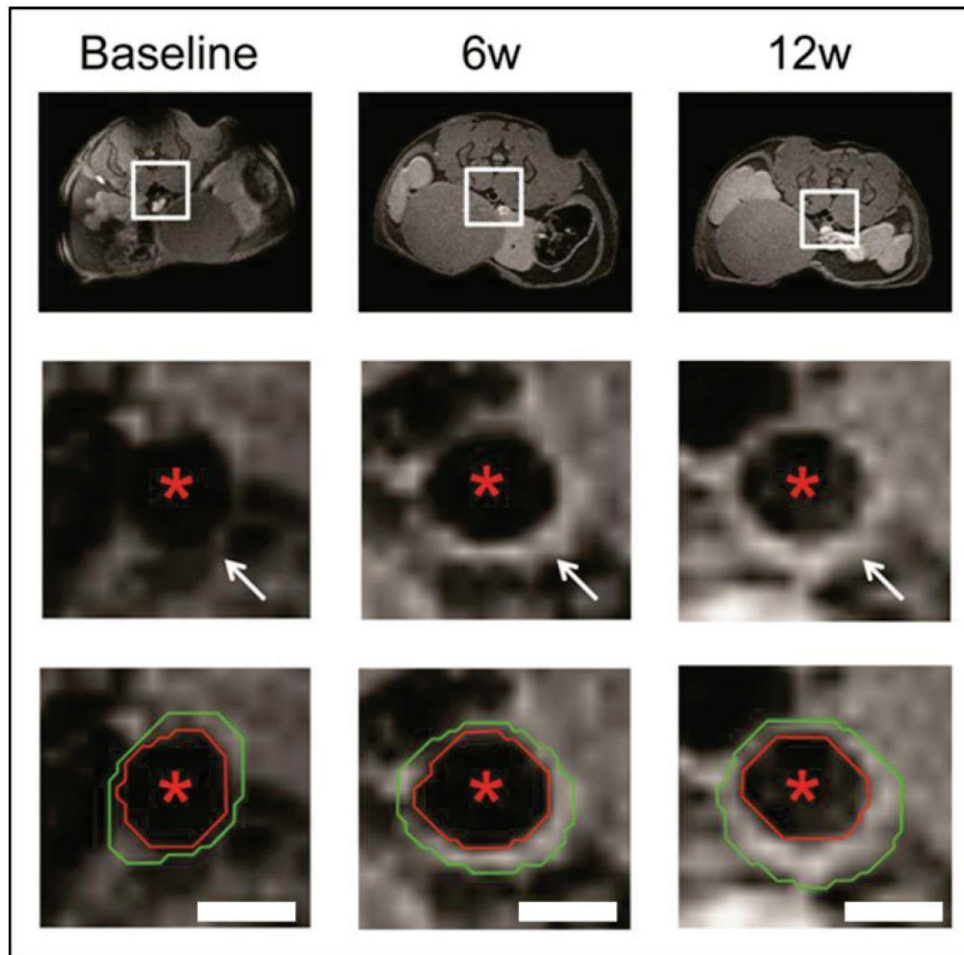
Supplementary Figure S7. [S]-rHDL targets Ly-6chi monocytes and macrophages in the spleen. (a) [S]-rHDL with the hydrophobic fluorescent dye DiO (red) in the core specifically targets CD68 (green) expressing monocytes and macrophages (islet) in the spleen. Cell nuclei are stained with DAPI (blue). (b) Macrophages and Ly-6c^{hi} (Gr-1^{hi}) monocytes took up [DiO-S]-rHDL most efficiently, while neutrophils and ly-6c^{lo} (Gr-1^{lo}) monocytes took up markedly less nanoparticles. Error bars are standard errors of the mean (N=3).



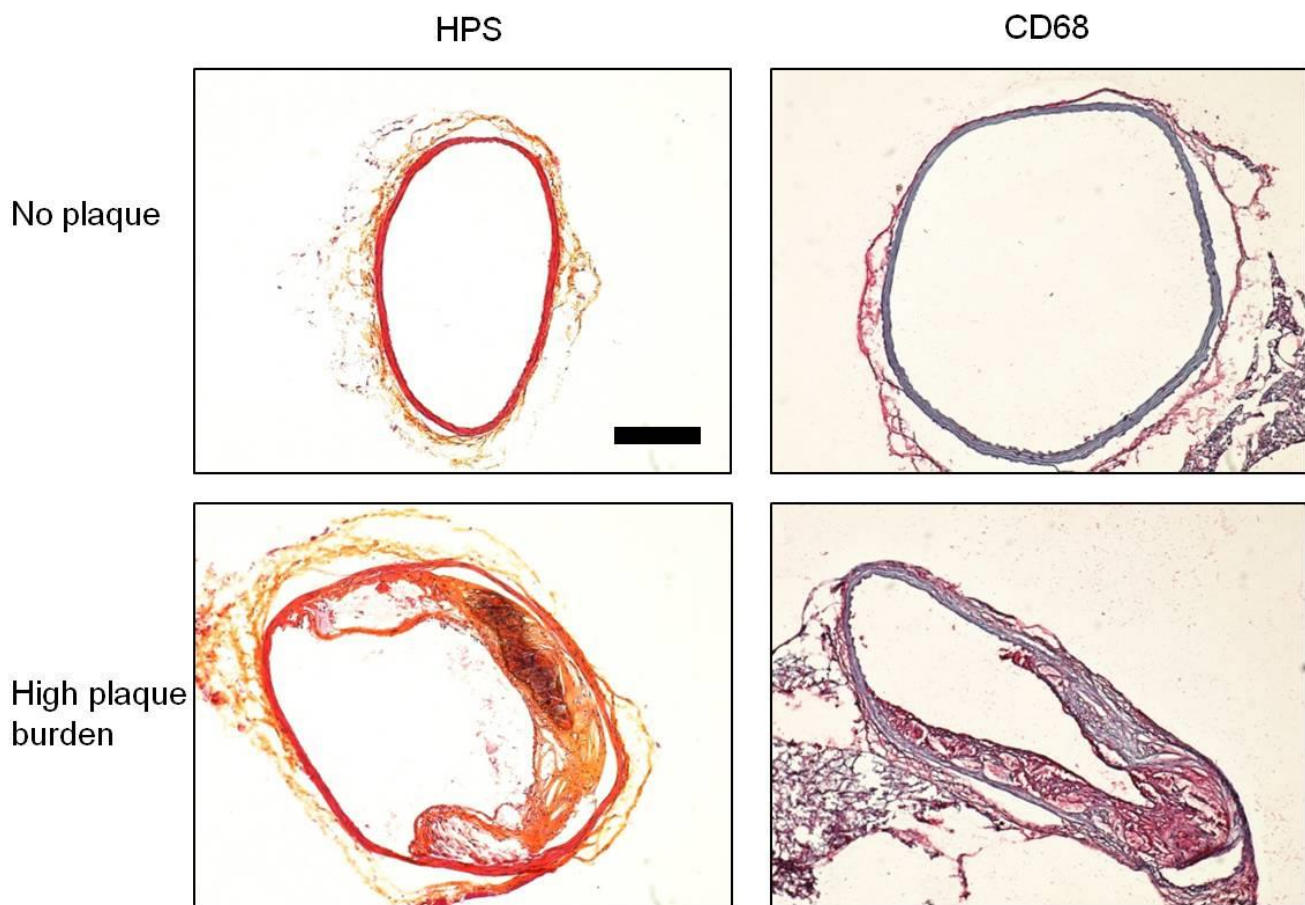
Supplementary Figure S8. Lack of toxic effects of one week high dose treatment. By the end of one week high dose [S]-rHDL treatment (60 mg/kg simvastatin, 40 mg/kg ApoA-1, 4 intravenous infusions /week), blood from [S]-rHDL treated (N=9) and placebo-treated (N=9) animals were collected, and serum was prepared as previously described. Toxic effects on liver were determined by measuring alanine transaminase (ALT) (a) and aspartate transaminase (AST) (b). Creatinine (c) is the marker for kidney damage, and creatine kinase (d) for muscle damage. Student t-test shows that high dose [S]-rHDL treatment does not produce significant toxic effects on liver, kidney, and muscle in these mice. Error bars are standard deviation, and Student t-test was used for statistical analysis.



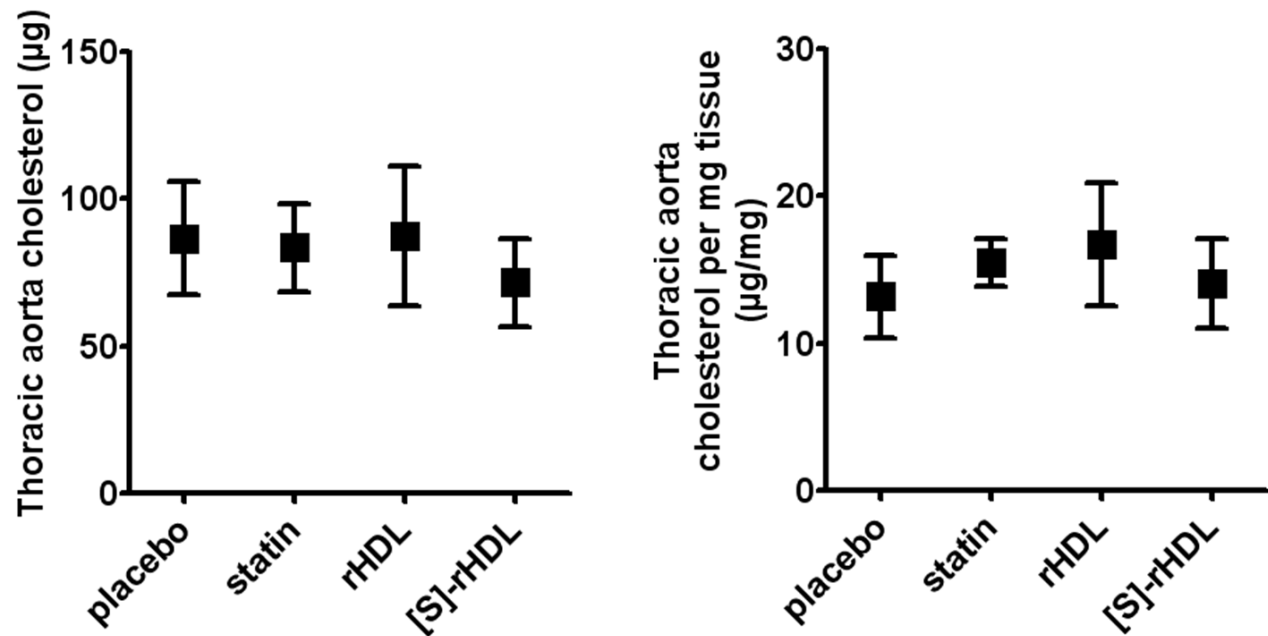
Supplementary Figure S9. Processing of histology images of the aortic sinus area with in-house developed software. Software written in Matlab was developed to facilitate automated image analysis. The analysis algorithm comprised subtraction of the back ground, followed by determination of cut-off values based on the colour histograms of each image, after which conversion to a binary image was made. Manual corrections could be made to mask out pixels outside the vessel wall. Mean plaque area was defined as the sum of the HPS area and CD68 area, and plaque macrophage area was defined as the CD68 positive area. The scale bar indicates 400 μ m.



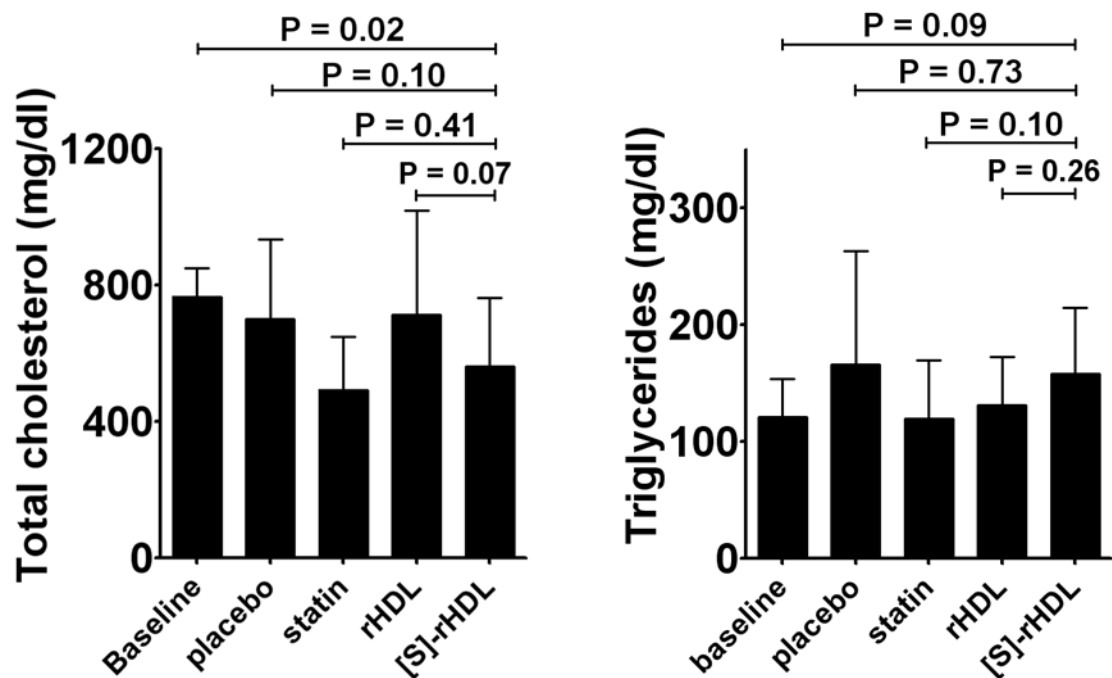
Supplementary Figure S10. Procedures to analyze MRI results from abdominal aortas. The white boxes indicate the location of the corresponding magnified images in the middle that show the abdominal aorta wall (white arrows). The analyzed images are shown at the bottom. The abdominal aorta lumen is indicated by *. The mean lumen area (LA), mean wall area (MWA) and mean outer wall area (OWA) of the images were calculated. Subsequently, the normalized wall index (NWI) was calculated by dividing the wall area by the outer wall boundary area, and used as the outcome parameter to describe the atherosclerotic burden of the abdominal aorta. Scale bars represent 500 μ m.



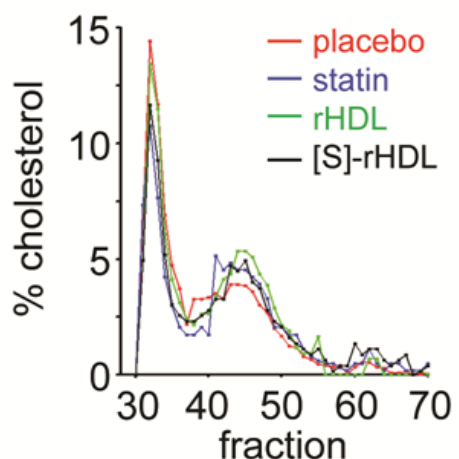
Supplementary Figure S11. Representative histology images of abdominal aortas. After MRI scanning, abdominal aortas were excised, sectioned, and stained with either HPS or CD68. The top images represent areas with no plaque, while the lower images depict areas with abundant plaques. Scale bar represents 200 μ m for all images.



Supplementary Figure S12. Cholesterol content. The cholesterol content of the thoracic aortas (including aortic arch) (left) and cholesterol content per milligram thoracic aorta tissue (right) of mice in the placebo (N=16), oral statin (N=15), rHDL (N=16), and [S]-rHDL long term treatment (N=15) groups. Cholesterol content and cholesterol content per milligram thoracic aorta tissue are similar in all groups. Bars represents 95% confidence intervals.



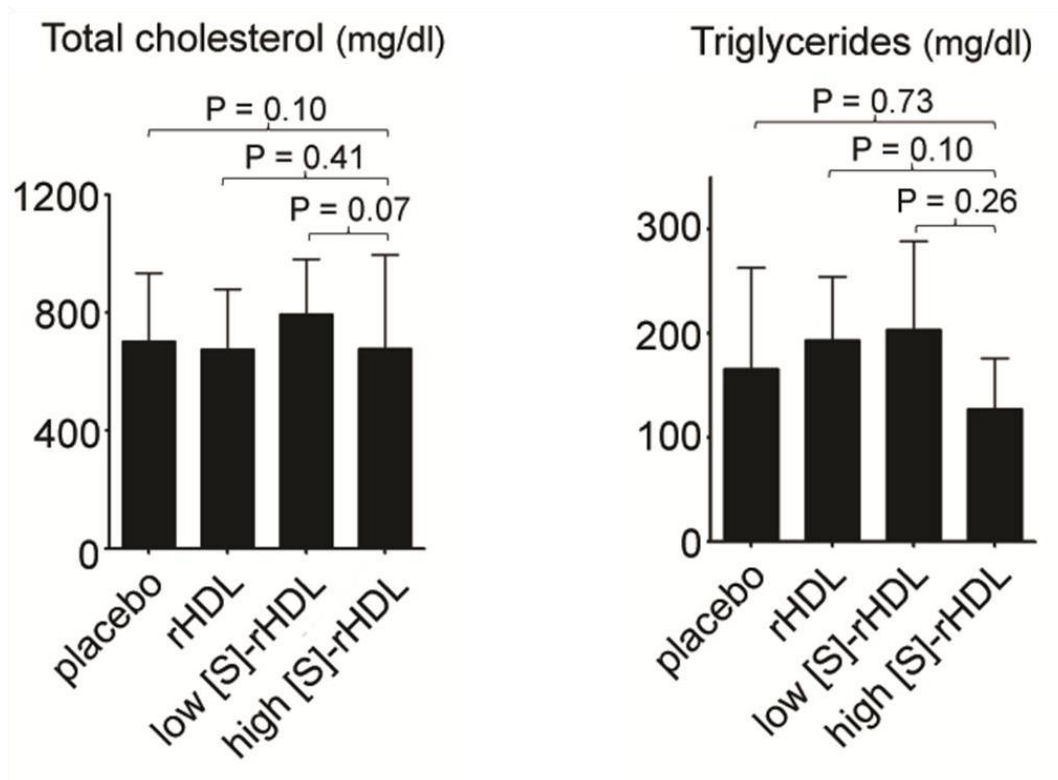
Supplementary Figure S13. Blood total cholesterol (left) and triglyceride (right) concentrations in blood of the mice that received 12 week treatment and for mice in the baseline group (N=12). Mice were sacrificed at the end of 12 weeks of treatment with placebo (N=16), statin (N=15), rHDL (N=16), [S]-rHDL (N=15), and blood was collected and total cholesterol and triglyceride levels were measured. P-values are calculated with Mann-Whitney U tests.



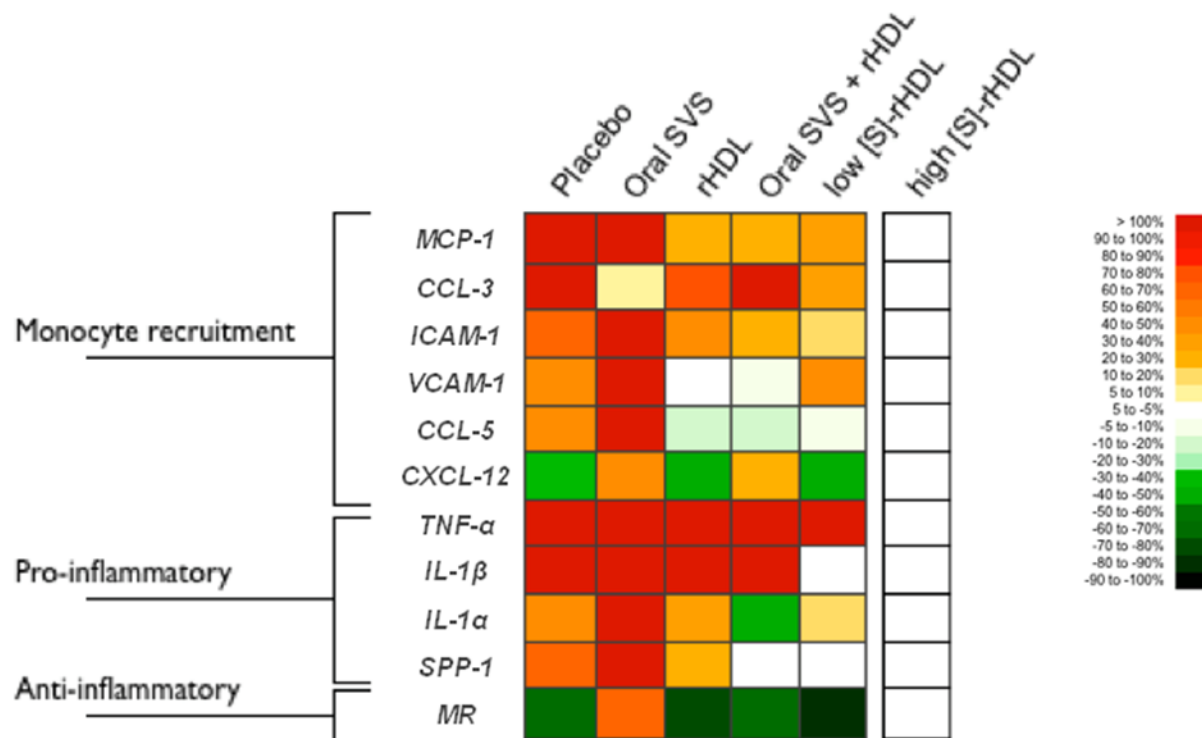
	VLDL (mg/dl, %)	LDL (mg/dl, %)	HDL (mg/dl, %)
placebo	399 (57)	300 (43)	18 (2)
statin	195 (39)	260 (52)	48 (9)
rHDL	296 (43)	379 (55)	24 (4)
[S]-rHDL	287 (44)	312 (48)	35 (5)

Supplementary Figure S14. Blood lipoprotein profile of mice receiving 12 weeks treatments.

Whole blood was obtained at the time of sacrifice by heart puncture of each mouse in each group, and plasma was prepared via centrifugation. The plasma samples of the same group were pooled for lipoprotein analysis via FPLC. The FPLC results show that in comparison to the [S]-rHDL group, the placebo and rHDL groups had a more atherogenic lipid profile, with a 112 mg/dl higher very low density lipoprotein cholesterol (VLDL) in the placebo group, and a 62mg/dl higher low density lipoprotein cholesterol (LDL-c) in the rHDL group. In The oral statin group had a more favourable lipid profile than the [S]-rHDL group, with 92 mg/dl lower VLDL, and 50 mg/dl lower LDL-c than [S]-rHDL treated group. The table shows the amount of cholesterol in the VLDL fractions (30-39), LDL fractions (40-56), and the high density lipoprotein fractions (57-63).



Supplementary Figure S15. Blood cholesterol (left) and triglyceride (right) levels of mice after receiving 1 week treatment with placebo (N=15), high dose rHDL (N=8), low dose [S]-rHDL (N=10), and high dose [S]-rHDL (N=10). P-values are calculated with Mann-Whitney U tests.



Supplementary Figure S16. This figure shows a heatmap of the percentage increase / decrease of plaque macrophage mRNA expression levels in the various treatment groups relative to the high dose [S]-rHDL group. The majority of the genes related to monocyte recruitment (Kruskal-Wallis for pooled analysis $P=0.001$), and pro-inflammatory genes (Kruskal-Wallis for pooled analysis $P=0.002$) increased relative to the high dose [S]-rHDL treatment group, while the anti-inflammatory mannose receptor gene expression showed a trend towards decrease in all groups except for the oral simvastatin (SVS) group (Kruskal-Wallis $P=0.07$).

Name	Phospholipids (w %)	ApoA-1 (w %)	Simvastatin (w %)	Gd-DTPA- DSA (w %)	Dye (w %)	Diameter by TME (nm)	Diameter by DLS (nm)	r1 (mM ⁻¹ . S ⁻¹)
[Gd-dye-S]- rHDL	19.5	6.5	9.8	19.5	2	20.5	29	9.9
[S]-rHDL	80.7	7.7	11.6	0	0	19.9	27	N/A
rHDL	71.4	28.6	0	0	0	10.6	12	N/A

Supplementary Table S1. Compositions of nanoparticles. Phospholipids, ApoA-1 proteins, simvastatin, Gadolinium-DTPA-DSA are shown in weight percentage (w %) of the nanoparticle. Dynamic light scattering (DLS) diameter was measured when nanoparticles were suspended in phosphate buffer saline, and transmission electron microscopy (TEM) diameter was measured when nanoparticles were negatively stained. The longitudinal relaxivity (r1) of [Gd-dye-S]-rHDL was measured at 60 MHz with a Bruker Minispec. Each measurement was performed in triplicate, and average values are shown here.